Quick Position Determination Using 1 or 2 LEO Satellites

NADAV LEVANON, Fellow, IEEE
Tel Aviv University

We describe an approach for a medium accuracy position determination of a user terminal (UT) on the Earth surface, using one or two low Earth orbit (LEO) satellites. The positioning approach is intended to meet the requirements of a worldwide personal communications system using LEO satellites. The basic two requirements are: 1) immediate positioning, and 2) horizontal position accuracy of the order of 10 km. Those requirements stem from the need of the system to know the user's approximate location before it connects his call. The approach makes use of the two-way communication with the UT, which can receive, transmit, and make its own measurements. Delay and Doppler measurements are used in order to enable instantaneous positioning with one satellite, and in order to achieve unambiguous positioning with two satellites. A simplified Globalstar satellite constellation and the expected Globalstar delay and frequency measurement accuracy are used to demonstrate the concept and to evaluate its performances.

Manuscript received September 12, 1996; revised July 31, 1997.

IEEE Log No. T-AES/34/3/06010.

This work was performed while the author was on sabbatical leave at Qualcomm Inc., 6455 Lusk Blvd., San Diego, CA 92121-2779.

Author's address: Dept. of Electrical Engineering–Systems, Tel Aviv University, P.O. Box 39040, Tel Aviv, 69978, Israel.

I. INTRODUCTION

A satellite-based personal communications system needs to know the caller's location in order to connect his call. This requirement is prompted by both operational needs such as territorial boundaries of the terrestrial service providers, as well as technical needs such as choosing the optimal gateway (GW). The acceptable positioning accuracy is not very strict—of the order of 10 km. What is critical is the delay in connecting the call, which should be in the order of few seconds. Since seeing only one satellite is sufficient for making a call, both requirements, accuracy and duration of the positioning process, should be met whether the user terminal (UT) sees one satellite or more.

The positioning approach described in this work can in most cases provide quick, medium accuracy positioning with one or more satellites. It makes use of the available two-way communication, as well as of the extensive Doppler shift associated with low Earth orbit (LEO) satellites. Clearly, different algorithms need to be used, and different performances should be expected in one versus two (or more) satellite cases. These distinctly different situations will result in different accuracy and also differ with regard to such issues as ambiguity and areas of accuracy singularities.

With regard to incoming calls, the system needs to know the user's approximate location in order to page him efficiently. Hence, a *mobile* UT needs to register even when it does not intend to place a call. Air-time used for registration bears no revenue. It can be minimized if the UT can determine passively (by just listening) how far it has traveled since its last registration and register only if a distance threshold was exceeded. A concept of passive positioning using two satellites is also described.

The Globalstar system [1] is used as an example (Fig. 1). The CDMA signal used in Globalstar allows relatively high accuracy delay measurements (it is a spread-spectrum signal as used in Global Positioning System (GPS)). Furthermore, the demodulation process requires frequency locking, which can double as an inherent frequency measurement. It should be pointed out however that Globalstar's prime mission is to provide a cost effective communication system. The navigation aspect serves internal needs. It could not justify additional dedicated circuitry, which would have improved the positioning accuracy.

The outline is as follows. Section II discusses existing dedicated satellite positioning systems. Section III explains our approach for quick, active, two-dimensional (2-D), single-satellite positioning. Section IV discusses 2-satellite positioning. Section V describes the iterative algorithm. Section VI presents simulation results on random error. Section VII discusses sources of bias error, including UT velocity.

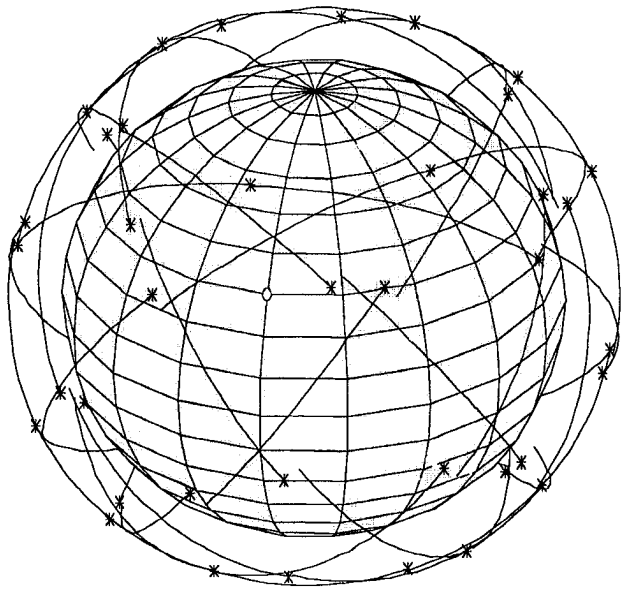

Fig. 1. 20 min trajectories of all 48 Globalstar satellites (Earth-fixed coordinates).

Section VIII presents the conclusions. Appendix B explains how Doppler is isolated from UT frequency offset. Appendix C discusses the effect of satellite orbit error.

II. EXISTING OPERATIONAL SATELLITE POSITIONING SYSTEMS

Several presently operational satellite positioning systems are briefly described. The systems differ in requirements and resources. Note that none of them achieves instantaneous positioning with only one satellite, as our approach does.

GPS [2] and GLONASS [2] are high accuracy, *one-way* systems (the user receives only), which require 4 simultaneous delay measurements from 4 satellites, in order to solve for the user's three position unknowns and for the user's clock offset. Two-dimensional positioning can be implemented with only 3 satellites in view. Because delay measurements are performed instantly, GPS or GLONASS position determination are not affected by user motion. Typical positioning accuracy of GPS, when using delay measurements, is 30 m.

The U.S. Navy TRANSIT [2] system (retired in 1996 after 34 years of outstanding service) is also a high accuracy *one-way* system. The user performs continuous Doppler-count type of frequency measurement (known also as integrated Doppler) of a signal received from a single LEO satellite. The measurements continue for several minutes. In addition to the three position unknowns, the receiver solves also for its own unknown reference frequency offset. Because it uses frequency measurements and because of the extended measurement period, TRANSIT is sensitive to user's motion and to his oscillator drift. In both GPS and TRANSIT the position calculation are performed at the user terminal. This requires broadcasting the satellites ephemeris. Typical accuracy of TRANSIT, using a single path, is 10 m.

ARGOS [3] and SARSAT (Search And Rescue SATellite) are two very similar medium accuracy systems using a single LEO satellite. Both can be described as *reverse one-way* systems. A user's beacon transmits periodic bursts of signals, and the satellite-borne receiver measures their frequency over an extended period of time (several minutes). A typical transmission duty-cycle is one second once every minute. Such a low duty-cycle is necessary in order to allow simultaneous tracking of many beacons. The number of frequency measurements exceeds the number of unknowns (= 4). The intermittent nature of the signal eliminates the option of an extended integrated Doppler measurement, which was an important contributor to the high positioning accuracy of TRANSIT. ARGOS and SARSAT are also sensitive to user's motion and oscillator drift. A mirror solution on the other side of the satellite subtrack satisfies the same measurements, except for a minor difference due to the Earth rotation. Many more measurements or external information is necessary to resolve that ambiguity. Typical accuracy of ARGOS is 500 m.

An example of an operational *two-way* position determination system is Qualcomm's OmniTRACS system [4, 5]. OmniTRACS positioning relies on two geostationary satellites. A round-trip delay measurement is performed through the communication link established through one satellite. A delay-difference measurement, performed on the signal received at the UT through the second satellite, provides the second required measurement for a 2-D positioning. An experimental system [6], similar to OmniTRACS, has also been reported. Typical accuracy of OmniTRACS is 300 m. In ARGOS, SARSAT, and OmniTRACS the positioning calculations are performed at a central ground station.

III. INSTANT SINGLE-SATELLITE POSITIONING

The number of Globalstar satellites, seen simultaneously by a UT, depends on latitude, time and the extent of sky blockage (buildings, trees). In order to be conservative, we assume that satellites are used for positioning, only down to 20° elevation angle. This intrinsically makes an allowance for blockage. With a 20° elevation angle mask, the probability of seeing only one satellite is rather high (Table I). Hence, being able to do single-satellite positioning is highly desirable. Table I was obtained from simulation of the Globalstar constellation, once every minute, over a period of 24 h.

TABLE I
Distribution of Number of Satellites Seen Simultaneously

Latitude	Number of simultaneous satellites visible above 20° elevation			
	0	1	2	3
0°	3 %	77 %	20 %	0 %
10°	11	57	32	0
20°	4	60	36	0
30°	0	43	55	2
40°	0	10	70	20
50°	0	19	71	10
60°	0	70	30	0
70°	75	25	0	0

Instant positioning using only one satellite becomes possible thanks to the two-way communication between the terrestrial gateway and the UT, and the capability of performing delay and frequency measurements at both ends. The single-satellite positioning is based on range and range-rate measurements.

A. Available Measurements

Range (RTD). A UT response to a received time mark, yields the round-trip delay (RTD). Subtracting the known GW-satellite delay, provides the satellite-UT range.

Range-Rate (RTDop). Assuming all the frequency conversions at the satellite relay are performed with known nominal local frequencies, and assuming perfect knowledge of the satellite position and velocity vector, allows for perfect correction of the satellite frequency conversions and for the GW-satellite Doppler shifts. What still prevents a measurement of the range-rate (the true Doppler in the satellite-UT link) is the unknown UT frequency offset. Appendix B describes a method (suggested by Steven A. Kremm [7]) to separate true Doppler from the UT frequency offset. This measurement is referred to as round-trip-Doppler (RTDop).

B. Simplified Physical Interpretation

The locus of all points on a spherical Earth which are at the same distance from the satellite is a circle. The locus of points with a given *range-rate* from the satellite is a cone whose origin is at the satellite, and whose axis of symmetry coincides with the satellite velocity vector. The cut between that cone and the surface of the Earth is hyperbola-like. Fig. 2 contains one iso-range circle and several iso-Doppler hyperbolas, labeled in kHz (corresponding to the Doppler shift at Globalstar's forward down-link carrier frequency of 2500 MHz). Fig. 2 demonstrates two difficulties which hamper such single-satellite positioning.

Ambiguity. For any UT position (e.g., the one marked in Fig. 2 at an intersection between the plotted iso-range circle and the +30 kHz hyperbola) there is clearly another point, symmetrically on the other side of the satellite subtrack, which also satisfies the same range and Doppler measurements. This is an unavoidable *ambiguity* problem.

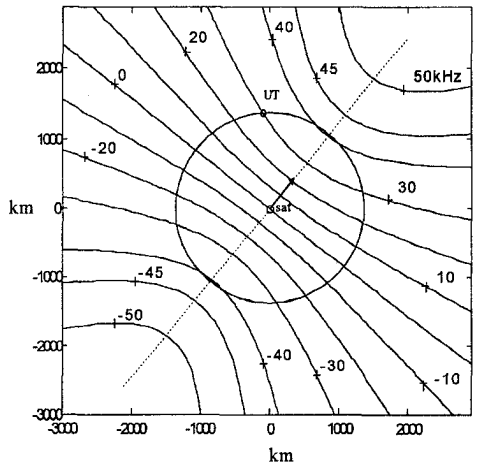

Fig. 2. Iso-range circle and iso-Doppler hyperbolas on Earth surface.

GDOP Singularity. For a UT location near the satellite subtrack (e.g., at the intersection between the circle and the +40 kHz hyperbola), the angle between the two contours becomes very small (nearly tangential). A measurement error will cause the intersection point to move drastically in a direction perpendicular to the subtrack. Such a strong dependence of the position solution on a measurement error is known as a large geometrical dilution of precision (GDOP). Exactly on the subtrack the GDOP peaks. Such a location is said to suffer from GDOP singularity.

The actual positioning algorithm does not attempt to draw a circle and a hyperbola and to find where they intersect. The positioning uses an iterative Newton algorithm. If there are additional measurements (e.g. due to a repetition of measurements) then an iterative weighted least-squares algorithm (Gauss–Newton) is used. The algorithm starts from an initial guess of the UT position. Using that guess it calculates the expected measurements and their derivatives with respect to

the two position unknowns (latitude and longitude). From the difference between the actual measurements and the calculated measurements and from the partial-derivative matrix, it obtains a correction to the initial position. The iterations continue until the solution converges (i.e., the correction becomes negligible).

Without external information, two measurements (range and Doppler) cannot resolve the ambiguity. The algorithm will converge to the solution on the same side of the subtrack where the initial guess was located. Repeated measurements are not going to help resolve the ambiguity, unless they are spaced well enough in time (in the order of a minute) to allow the Earth rotation to cause enough lack of symmetry, that can be detected with the available measurement accuracy. External sources of information that can resolve ambiguity are 1) the satellite antenna beam on which the signal was received, 2) previous known position, and 3) stored old measurements made at the UT from a *pair* of satellites.

If the UT position is near a GDOP singularity, or if ambiguity could not be resolved, then positioning cannot be determined. Position determination will have to be delayed until the geometry has improved, or more measurements have been accumulated, or a second satellite has appeared.

Fig. 2 provides also some hints about relating measurement errors to the resulting position error. Consider an intersection where the circle and the hyperbola are perpendicular, e.g., the crossing point between the circle and the 0 kHz hyperbola. At that point the *along-track* position error is solely determined by the frequency measurement error. Note that there is 330 km horizontal distance spacing between hyperbolas spaced 10 kHz apart. This implies a sensitivity of 33 m/Hz in the along-track direction at that particular location. The error in the *across-track* direction at that point is solely determined by the error in the slant range (delay) measurement. At that particular point the UT-satellite slant range is approximately 2000 km and the horizontal range is approximately 1400 km, hence the error sensitivity in the across-track direction is 1.4 m/m.

At other locations the sensitivity to measurement error is more complex to calculate. However, from Fig. 2 we can still note the trends. The sensitivity to frequency error increases away from the satellite subpoint, while the sensitivity to range measurement error increases closer to the subpoint.

The expected corresponding measurement errors in the Globalstar system are $\sigma_R = 40$ m and $\sigma_{f_D} = 30$ Hz (resulting from two frequency measurements). These numbers are not a result of any physical limitation, but of the available circuitry in the Globalstar system, which was not designed with positioning accuracy in mind. For example the $\sigma_R = 40$ m accuracy is due in part to the clock resolution which is 1/8th of a PN chip. (The chip duration is 0.813 μs which corresponds to 244 m.)

The expected RTD measurement error $\sigma_R = 40$ m, and RTDop error $\sigma_{f_D} = 30$ Hz, combined with the two sensitivity numbers obtained from Fig. 2, (33 m/Hz and 1.4 m/m) will cause corresponding position errors of 56 m and 1000 m, respectively.

Such very unbalanced errors suggest that if higher positioning accuracy is desired, it is worthwhile to devote an effort to improve the frequency measurement. If the frequency measurement error could be reduced to few Hz, then the errors will be comparable.

C. Comparison with Two-RTD Positioning

Without frequency measurement, single-satellite positioning could be implemented using two RTD measurements spaced τ seconds apart. The change of range during τ is the equivalent of range-rate. How long need τ be, in order to obtain the same accuracy of range-rate, as the accuracy obtained from Doppler measurement?

From the relationship between range-rate and Doppler

$$\dot{R} = -\lambda f_D \tag{1}$$

where λ is the wavelength ($\lambda = 0.12$ m), we get

$$\sigma_{\dot{R}} = \lambda \sigma_{f_D}. \tag{2}$$

From the relationship between range-rate and two range measurements

$$\dot{R} \approx \frac{R(t) - R(t-\tau)}{\tau} \tag{3}$$

we get

$$\sigma_{\dot{R}} = \frac{\sigma_R \sqrt{2}}{\tau}. \tag{4}$$

Equating (2) and (4) yields

$$\tau = \frac{\sigma_R \sqrt{2}}{\lambda \sigma_{f_D}}. \tag{5}$$

Using $\sigma_R = 40$ m and $\sigma_{f_D} = 30$ Hz, (5) yields $\tau =$ 16 s. Waiting 16 s to complete the positioning measurements cannot be considered instant positioning.

D. Height-Induced Error in Single-Satellite Positioning

The single-satellite positioning described above assumed that the UT is on the Earth surface (or that its height above the Earth surface is known). Since only two measurements are available, only the two horizontal position coordinates can be estimated. In this section we evaluate the effect of an error in the assumed UT height.

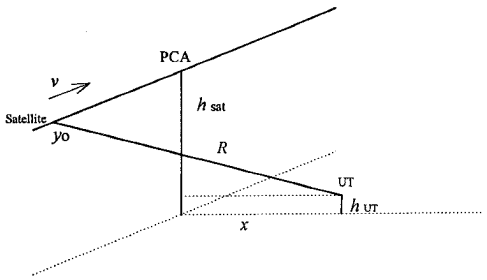

Fig. 3. Satellite-UT geometry for flat stationary Earth model.

The geometrical coupling of an error in the assumed height to a horizontal position error, for a one-satellite case, can be easily demonstrated with a flat and stationary Earth model. The satellite is assumed to have a fixed velocity v, and its motion is along a straight line, at a constant height h_{sat} above the flat Earth surface. The UT horizontal position unknowns (relative to the satellite) are the across-track distance x, and the along-track distance y_0, measured from the point of closest approach (PCA). The cause of the horizontal position error is an error Δh in the height h_{UT}.

Fig. 3 indicates that the range is given by

$$R(t) = \sqrt{x^2 + (h_{\text{sat}} - h_{\text{UT}})^2 + (y_0 - vt)^2}. \tag{6}$$

The range-rate is given by

$$\dot{R}(t) = -\frac{v(y_0 - vt)}{\sqrt{x^2 + (h_{\text{sat}} - h_{\text{UT}})^2 + (y_0 - vt)^2}}. \tag{7}$$

Note that in both equations, x and h_{UT} are coupled together in the expression $x^2 + (h_{\text{sat}} - h_{\text{UT}})^2$. Hence, it is actually this expression that is estimated instead of the across-track parameter x by itself. This implies that an error in h_{UT} will cause an error only in x.

Defining the UT height error as Δh, and the resulting position error (in the *across*-track direction x) as Δx, we can write

$$x^2 + (h_{\text{sat}} - h_{\text{UT}})^2 = (x + \Delta x)^2 + (h_{\text{sat}} - h_{\text{UT}} - \Delta h)^2. \tag{8}$$

Assuming small errors ($\Delta x \ll x$, $\Delta h \ll h_{\text{sat}} - h_{\text{UT}}$), (8) reduces to

$$\Delta x \approx \Delta h \frac{h_{\text{sat}} - h_{\text{UT}}}{x} \approx \Delta h \frac{h_{\text{sat}}}{x}. \tag{9}$$

Equations (6)–(9) imply the following. 1) In a flat Earth model, an error in the assumed UT height will result in a positioning error only in the across-track direction x. 2) The error Δx is of the order of the error Δh in the assumed height, when the distance of the UT from the satellite subtrack x is about equal to the satellite height above the Earth surface h_{sat} (= 1400 km). 3) The height-induced positioning error increases as the UT gets closer to the subtrack (smaller x). Simulations with a spherical Earth model confirmed the relationship in (9).

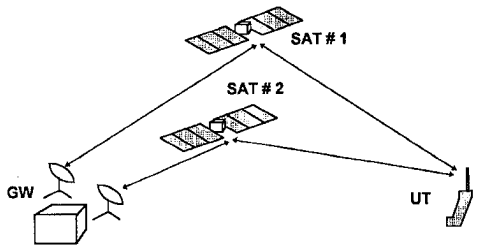

Fig. 4. System components is two-satellite positioning.

Using a detailed digital topographic map it is possible to reduce the height induced error. Once the positioning algorithm has converged (assuming a simple smooth Earth model, e.g., WGS-84), the terrain height at that location will be used as a more correct height assumption, and the positioning will be redone. Several iterations of this kind are possible.

IV. TWO-SATELLITE POSITIONING

Positioning accuracy can be drastically improved when the UT receives signals from two satellites (Fig. 4). With two satellites the ambiguity problem and GDOP singularities practically disappear. Receiving two satellites adds two more measurements as follows.

Range-Difference (Δt). This is obtained from the delay difference Δt, between the signals received from the two satellites. Note that the GW precorrects for each GW-satellite delay, so that the transmissions from all satellites are synchronized.

Doppler-Difference (Δf). The GW also precorrects for each GW-satellite Doppler shift, so that the carrier signal transmitted by all satellites is at the nominal forward frequency. The UT measures the frequency difference between its local reference and each received signal. Hence the frequency difference corresponds to the true Doppler difference, Δf.

While all four measurements (RTD, Δt, Δf, and RTDop) should be available from two satellites, a single figure with the contour families of all four measurements is too crowded to be meaningful. Hence, the physical interpretation considers three measurements at a time.

A. Positioning Based on RTD, Δt, and Δf Measurements

The information in the first three measurements creates three families of contours on the Earth surface, as depicted in Fig. 5. The figure contains also the subpoints of the two satellites (marked as sat #1 and sat #2). The arrows emanating from the two satellite subpoints indicate their direction of motion. The

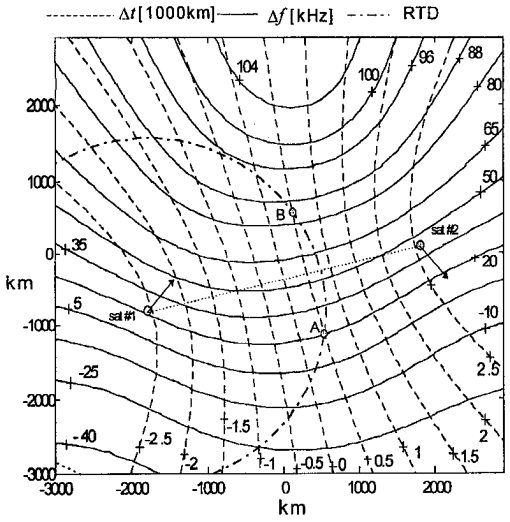

Fig. 5. Typical RTD, Δt, and Δf contours.

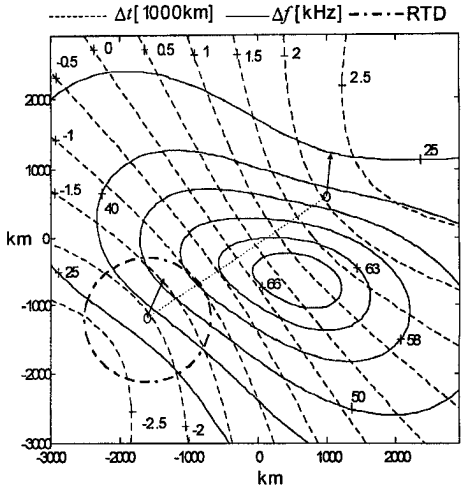

Fig. 6. Bad GDOP scenario of RTD + Δt + Δf.

present baseline is the dotted line connecting the two satellite subpoints. Contrary to the relatively fixed subtrack of a single satellite, the two-satellite baseline is changing rapidly. The three types of contours are the following.

RTD. An RTD measurement is performed only with respect to one satellite—the one on which the two-way communication is established. The locus of points on the Earth surface with a given distance to the satellite, is a *circle*. Only one such circle (dash–dot) is plotted in Fig. 5. It represents a satellite-UT slant range of 2750 km.

Δt. The locus of points on the surface of the Earth with the same range-difference from two satellites, is hyperbola-like. The hyperbolas (dashed lines) cross the baseline, connecting the two satellite subpoints, at 90°. Eleven such hyperbolas are shown in Fig. 5. The label represents the range-difference in units of 1000 km. The central hyperbola (a normal bisector of the baseline) is labeled 0. Its right-hand neighboring hyperbola, labeled 0.5, indicates that the distance from a UT located on it to satellite #1 is 500 km longer than the distance from that UT to satellite #2.

Δf. The locus of points (solid lines) on the surface of the Earth, of all locations which receive a given Doppler-difference from the two satellites, has no universal shape. The Δf contours depend on both the positions and the velocity vectors of the two satellites. The labels are in kHz. The highest Δf contour in Fig. 5 is 104 kHz. It surrounds an area around $X = 0$ and above $Y = 2000$ km. Note that the velocity vector of satellite #1 points toward that area, while the velocity vector of satellite #2 points away from it. The Doppler difference would therefore be nearly twice the maximum individual Doppler shift. Depending on the minimum usable satellite elevation above the horizon, the 104 kHz contour may be out of range of the two satellites simultaneously.

Fig. 5 demonstrates that if only RTD + Δt measurements were used, any intersection between the RTD circle and a Δt hyperbola has a corresponding mirror intersection (e.g., points A and B) which satisfies the same measurements. Hence positioning based on RTD + Δt suffers also from *ambiguity*. The addition of the Δf contours clearly resolves that ambiguity. The Doppler-difference at point A is 20 kHz, while at point B it is 84 kHz. It should be emphasized that in implementing the positioning algorithm, by an iterative weighted least-squares algorithm (e.g., Gauss–Newton), all measurements are used simultaneously, and the algorithm can be made to converge automatically to the correct solution no matter where the first guess was. The positioning algorithm is discussed in more details in Section V.

Near the baseline, an RTD circle must be tangential to the relevant Δt hyperbola, since both intersect the baseline at a 90° angle. A small error in either measurement will shift the solution drastically in a direction normal to the baseline. Hence positioning based on RTD + Δt suffers also from *GDOP singularity*. However, in that same area, an intersection between an RTD circle (or a Δt hyperbola) and a Δf contour is very favorable (i.e., almost perpendicular). This implies that near the baseline, the least-squares algorithm will automatically let the Δf measurement determine the across-baseline coordinate of the solution, and a GDOP singularity will be avoided.

B. Rare Situation When Δf By Itself Cannot Mitigate RTD + Δt GDOP Singularity

The example in Fig. 6 occurs when the UT sees two satellites moving in nearly parallel directions. This can usually happen when the two satellites belong to two consecutive orbits. Both satellites are necessarily at low elevation, with one satellite in the opposite side of the UT than the other.

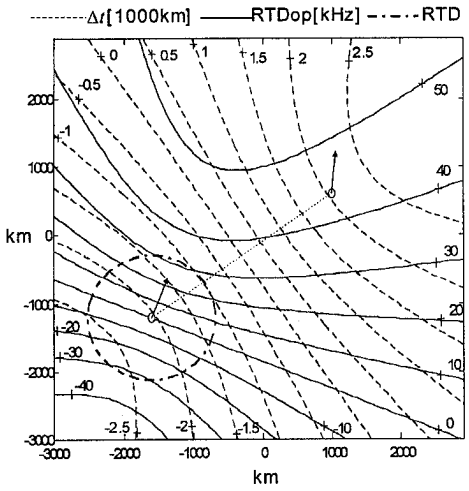

Fig. 7. RTD, Δt, and RTDop contours for same geometry as Fig. 6.

Nearly parallel velocity vectors create drastically different Δf contours. In between the two satellites, where a UT can be seen by both of them simultaneously, the Δf contours are *closed* contours. Each Δt hyperbola and each RTD circle now intersect the same Δf contour *twice*. Such a scenario can create a tri-way poor GDOP situation. Note how the 58 kHz Δf contour and the -1 (thousand km) Δt contour are both tangential to the RTD contour. This is where the additional RTDop measurement becomes important, as is demonstrated in the next section.

C. Positioning Based on RTD, Δt, and RTDop Measurements

Replacing the Δf contours with true Doppler contours (obtained from the RTDop measurement) creates the three families of contours in Fig. 7. The Doppler contours (solid lines) represent the Doppler frequency of the signal received at the UT from satellite #1. They are labeled in kHz. The Doppler contours are hyperbola-like, symmetric with respect to the velocity vector of the relevant satellite. The satellite constellation in Fig. 7 is identical to the satellite constellation in Fig. 6. Note that the RTDop contours do mitigate the RTD + Δt GDOP singularity (the tangential point between the RTD circle and the Δt contour labeled -1).

If RTDop measurement where to *replace* the Δf measurement, the positioning accuracy would have degraded somewhat. If RTDop is *added* to the Δf measurement, then the positioning accuracy will further increase due to the added redundancy. In a two-satellite situation both type of measurements should be available.

The added redundancy of using both types of Doppler measurement is further useful in those rare cases when each one by itself cannot mitigate bad GDOP or resolve ambiguity.

D. Passive Two-Satellite Positioning, Using Δt and Δf

As pointed out in the introduction, distance-based registration will reduce the air-time overhead of the system. The UT will reregister only if it had traveled significantly away from its previously registered position. The accuracy requirements and the acceptable delay in obtaining the position are even more relaxed for this application. In order to implement such a concept the UT has to be able to determine its own position by passively receiving satellite signals. Passive positioning requires a minimum of two satellites, from which two passive measurements are available $-\Delta t$ and Δf. Since the exact time in which the UT obtains these measurements and calculates its position is not very critical, waiting several minutes for a two-satellite scenario to materialize is tolerable.

The physical interpretation of these two measurements can be deduced from Fig. 5 by disregarding the RTD circle. Note from Fig. 5 that the intersections between the Δt and Δf contours are generally favorable, with no ambiguities or bad GDOP. However, the scenario depicted in Fig. 6 can also occur (albeit rarely). Ignoring the RTD circle in Fig. 6, we note both ambiguity problems (where a Δt contour intersects the same Δf contour at two different places) and bad GDOP areas (where a Δt contour is nearly tangential to a Δf contour). Regarding GDOP, since GDOP is calculated as part of the positioning algorithm, a bad GDOP situation can be discarded, and the UT can wait for a different two-satellite geometry. Regarding ambiguity, the UT will always use his last registered position as a first guess. If it did not travel a large distance away, then this first guess is likely to lead the algorithm to converge to the true solution. If it did travel a great distance from the last registration, then it is supposed to reregister anyway. Hence converging to either the true or the mirror solution will result in the same outcome, reregistration. Registration automatically prompts the more accurate active positioning.

V. POSITIONING ALGORITHM (TWO-DIMENSIONAL)

An M-dimensional vector of measurements denoted $\mathbf{z}$ is available. It consists of all or some of the following measurements: delay (range), delay difference, Doppler (range-rate) and Doppler-difference. The measurements are nonlinear functions of the 2-dimensional UT position vector $\mathbf{x}$

$$\mathbf{x} = [\text{lat long}]^T \tag{10}$$

according to

$$\mathbf{z} = \mathbf{h}(\mathbf{x}) + \mathbf{v} \tag{11}$$

where the M-dimensional vector $\mathbf{v}$ represents the measurement errors. Following Gauss' method of linearization we use the $(M \times 2)$ partial derivative matrix $\mathbf{H}$, whose (m,k) element is the partial derivative of the mth measurement with respect to the kth position parameter, calculated at a given position $\mathbf{x}$

$$\mathbf{H} = \mathbf{H}(\mathbf{x}) = \frac{\partial \mathbf{h}}{\partial \mathbf{x}}(\mathbf{x}) \tag{12}$$

and apply an iterative weighted least-squares algorithm (weighted Gauss–Newton method) [8] to solve for the unknown position parameters:

$$\hat{\mathbf{x}}_{i+1} = \hat{\mathbf{x}}_i + (\hat{\mathbf{H}}^T \mathbf{W} \hat{\mathbf{H}})^{-1} \hat{\mathbf{H}}^T \mathbf{W}(\mathbf{z} - \hat{\mathbf{z}}) \tag{13}$$

$\hat{\mathbf{x}}_i$ and $\hat{\mathbf{x}}_{i+1}$ are the current and next estimates, respectively. The subscript i represents the iteration number, with $i = 0$ representing the first guess

$$\hat{\mathbf{H}} = \mathbf{H}(\hat{\mathbf{x}}_i) \tag{14}$$

is the partial derivative matrix calculated at the current position estimate, and

$$\hat{\mathbf{z}} = \mathbf{h}(\hat{\mathbf{x}}_i) \tag{15}$$

are the expected error-free measurements, calculated using the current position estimate. The iterations terminate when the correction from $\hat{\mathbf{x}}_i$ to $\hat{\mathbf{x}}_{i+1}$ becomes negligible.

The elements of the $M \times M$ weight matrix $\mathbf{W}$ provide means to emphasize the influence of specific measurements upon the estimated parameters $\hat{\mathbf{x}}$. Optimal accuracy is obtained if the weight matrix is chosen as the inverse of the measurement error covariance matrix.

If the measurement errors are mutually independent with zero mean and variances

$$\sigma_m^2, \qquad m = 1,2,\ldots,M \tag{16}$$

then $\mathbf{W}$ is a diagonal matrix with σ_m^{-2} as its diagonal elements.

With this choice of $\mathbf{W}$ the variance of the kth element of the estimated unknowns vector $\mathbf{x}$ is given by

$$\sigma_k^2 = (\mathbf{H}^T \mathbf{W} \mathbf{H})_{k,k}^{-1}, \qquad k = 1,2. \tag{17}$$

Recall from (10) that $k = 1$ corresponds to latitude and $k = 2$ corresponds to longitude.

Finally, the combined theoretical horizontal position error, in units of distance, is given by

$$\sigma_{\text{pos}} = R_{\text{E}} \sqrt{\sigma_1^2 + \sigma_2^2 \cos^2(\text{lat})} \tag{18}$$

where R_{E} is the Earth radius. This theoretical positioning error is the equivalent of the GDOP multiplied by the standard deviation of the measurement error, when only one kind of measurement is used (e.g., delay measurements in GPS).

In two-satellite positioning, which uses both delay and Doppler measurements, optimal accuracy is achieved when the weight matrix is chosen as the inverse of the measurement error covariance matrix. However, with such a weight matrix the least-squares cost function

$$l_{\text{LS}} = [\mathbf{z} - \mathbf{h}(\mathbf{x})]^T \mathbf{W} [\mathbf{z} - \mathbf{h}(\mathbf{x})] \tag{19}$$

may look as in the top part of Fig. 8 (pertains to two-satellite positioning using RTD + Δt + Δf). This cost function exhibits a deep minimum at the correct solution but also an additional strong local minimum at the mirror location of the RTD + Δt solution. The iterative algorithm descends the slope of the cost function. Depending on the initial guess, it can converge to the wrong local minimum (the mirror solution). Recall from Fig. 5 that the arbiter between the two solutions is the frequency measurement Δf. With the optimal weight matrix, the local minimum at the mirror solution is raised but not eliminated. However, if frequency is given much more weight, the additional local minimum completely disappears as depicted in the lower part of Fig. 8.

A practical approach that guarantees convergence to the correct solution with the minimum possible error, is to change the weight matrix $\mathbf{W}$ during the iterative process. The algorithm starts with a $\mathbf{W}$ matrix which emphasizes frequency measurements. This will steer the outcome of the first iterations toward the correct solution (rather than the mirror solution of RTD + Δt) no matter where the first guess is. Only at a later iteration the algorithm switches to the optimal $\mathbf{W}$ in order to achieve the smallest possible random error (statistically).

Instead of using *latitude* and *longitude*, the UT position can be defined using 3 Cartesian coordinates. In that case an additional constraint (perfect measurement) is added; their sum of squares should be equal to the square of the Earth radius.

The vector of unknowns $\mathbf{x}$ may have to include nuisance parameters as well. For example, in single-satellite positioning, if instead of calculating the range-rate beforehand, from the two frequency measurements at the GW and at the UT (see (25) in Appendix B), the algorithm uses these two measurements as individual measurements, then the vector of unknowns has to include the UT frequency offset as an additional nuisance unknown, which is related to the two measurements according to (26).

VI. RANDOM POSITIONING ERRORS

Random error is caused by noise induced random measurement errors. σ_{pos} the random error standard deviation (STD) can be calculated using the theoretical error expression given in (18). Clearly, it is a function of the geometry between the satellite

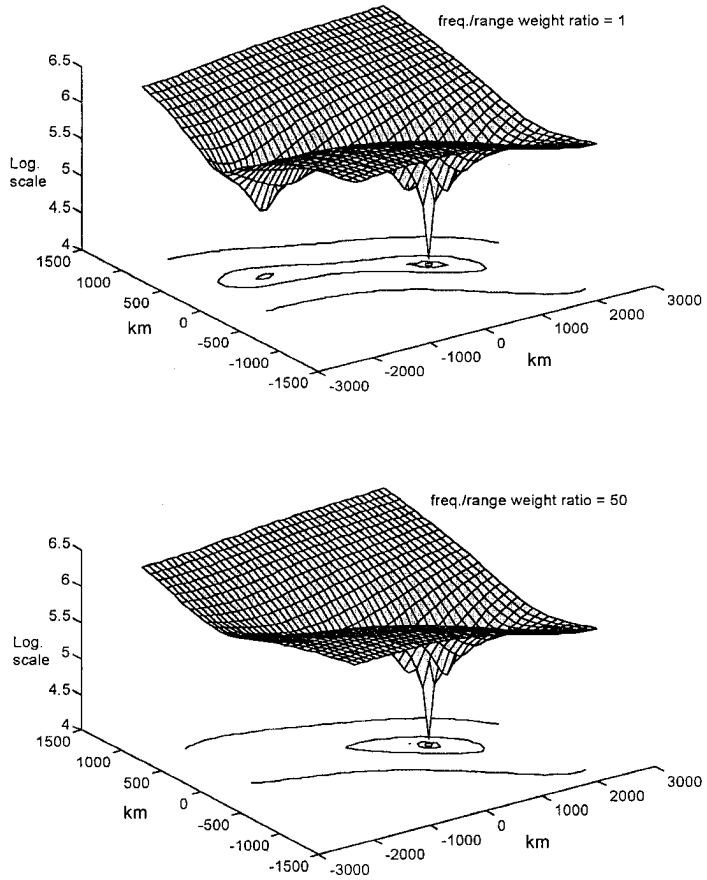

Fig. 8. Two least-squares cost functions with different weight matrix W (2-satellite positioning using RTD + Δt + Δf).

constellation and the UT. The statistical distribution of σ_{pos}, for a given UT location, can be obtained from simulating the time-changing Globalstar constellation at small time intervals, and at each instance calculating σ_{pos}. A histogram of calculations performed once a minute over 24 h provides a good representation of the probability density function (pdf) of σ_{pos}. The statistics are a function of latitude.

Only satellites above an elevation of 20° were considered. The simulation results are presented for a UT at a 30° latitude, which corresponds approximately to the middle of Globalstar's latitude coverage band in each hemisphere. The distribution of the number of satellites seen simultaneously above 20° elevation, at various latitudes appeared in Table I.

The theoretical calculations presented in the next sections assumed Gaussian measurement errors with zero mean and STD of 40 m for range (delay) measurements and 30 Hz for frequency measurements (at both the GW and at the UT). These are the measurement error STDs expected in Globalstar.

A. Random Error. Single-Satellite Positioning (RTD + RTDop)

The cumulative distribution function (cdf) of the σ_{pos} calculations, for a *single-satellite* positioning of a UT at 30° latitude, is presented in Fig. 9. Scenarios with N simultaneous satellites were treated as N single-satellite cases.

Note that σ_{pos} can never be zero, even at the lowest (best) possible GDOP. The cdf curve indicates that with the assumed measurement errors, single-satellite random positioning error will exceed 14.5 km in only 6% of the cases, while the median error is 2.5 km. The remaining 6% represent the tail of the pdf which may extend to very large error values representing GDOP singularity cases.

The major differences between the performances in different latitudes are mostly due to the changing mix of single- and two-satellite cases. Since Fig. 9 represents only single-satellite cases, the results for other latitudes will be similar. There are however two exceptions.

1) At and near the specific latitude of 52 deg, which corresponds to the Globalstar orbit inclination, the probability of overhead path is relatively high. For single-satellite positioning, this means many cases in which a UT (at latitude of 52°) will be on or near the satellite subtrack, which results in GDOP singularity.

2) At latitudes higher than 52°, overhead path can never occur, hence there will be no GDOP singularities and the tail of the pdf will not extend as far as in Fig. 9. For example at 60° latitude the

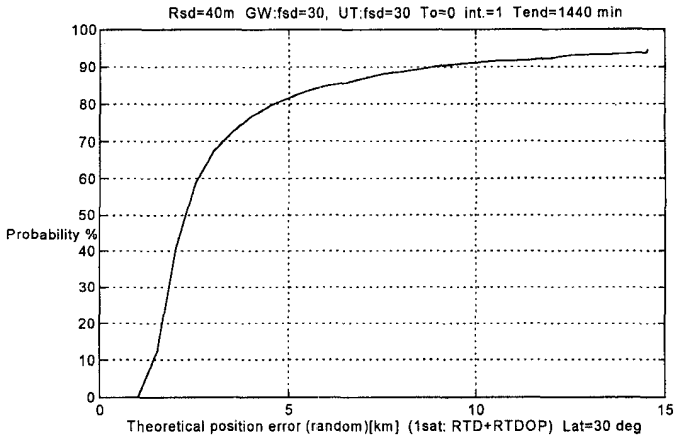

Fig. 9. CDF of theoretical STD of random positioning error using single satellite.

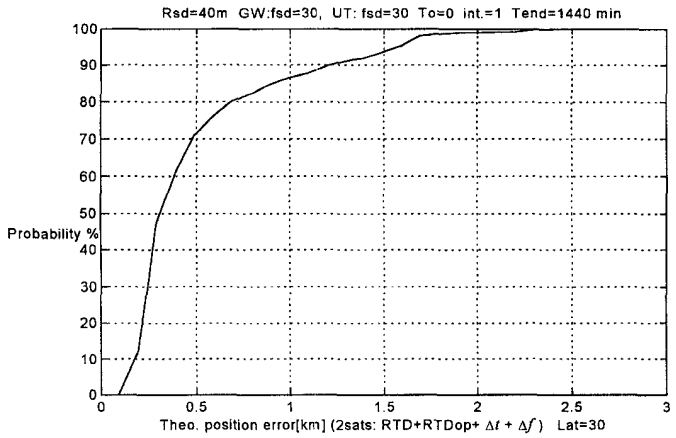

Fig. 10. CDF of theoretical STD of random positioning error using two satellites.

cdf reaches 100% for an error smaller than 15 km. However, at that latitude the probability of seeing two satellites simultaneously drops to only 30%.

B. Random Error. Two-Satellite Active Positioning (RTD + RTDop + $\Delta t + \Delta f$)

The cdf of σ_{pos}, for *two-satellite* positioning of a UT at 30° latitude, is presented in Fig. 10. Scenarios with 3 simultaneous satellites were treated as 3 two-satellite cases. Note the reduced error, as well as lack of GDOP singularities. The pdf tail ends at an error of 2.3 km, with a median error of 0.3 km. Had we used only delay measurements (RTD + Δt), GDOP singularities would have been observed.

Fig. 11 demonstrates the contribution of the two Doppler measurements (RTDop + Δf) toward eliminating GDOP singularities. For each two-satellite case the theoretical error was calculated twice, once for using delay measurements only (RTD + Δt) and once for using all 4 measurements (RTD + RTDop + $\Delta t + \Delta f$). Fig. 11 displays all the relationships between the two errors accumulated over 24 h. Note that while positioning based on RTD + Δt exhibits quite a few bad GDOP cases (in which the error exceeds 3 km, for example), adding the Doppler measurements bounds the error in these cases to less than 2.3 km. On the other hand, note that in the good GDOP cases of RTD + Δt positioning (error less than 0.5 km), the Doppler measurements hardly add any accuracy. It is in these good GDOP cases of RTD + Δt, that the Doppler measurements are important for their other role of resolving the ambiguity inherent in RTD + Δt positioning.

C. Random Error. Two-Satellite Passive Positioning ($\Delta t + \Delta f$)

In passive positioning the UT only receives. Round-trip measurements cannot be performed and the only available measurements are Δt and Δf.

The cdf of σ_{pos}, for *two-satellite passive* positioning of a UT at 30° latitude, is presented in Fig. 12. Here scenarios with 3 simultaneous satellites were treated as 3 different combinations of two-satellite cases.

Loosing the RTD measurement turns out to be costly as far as accuracy is concerned. The median positioning error in two-satellite *passive* positioning increases to 2.5 km, and GDOP singularities reappear (in 6% of the cases the error will be larger than

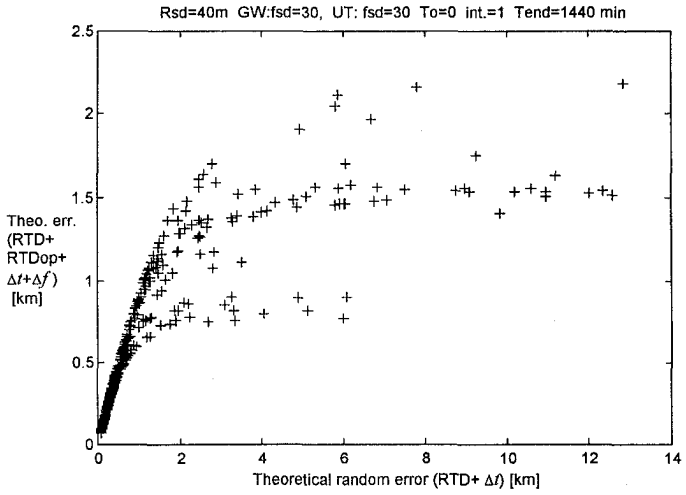

Fig. 11. Effect of Doppler measurements on two-satellite positioning.

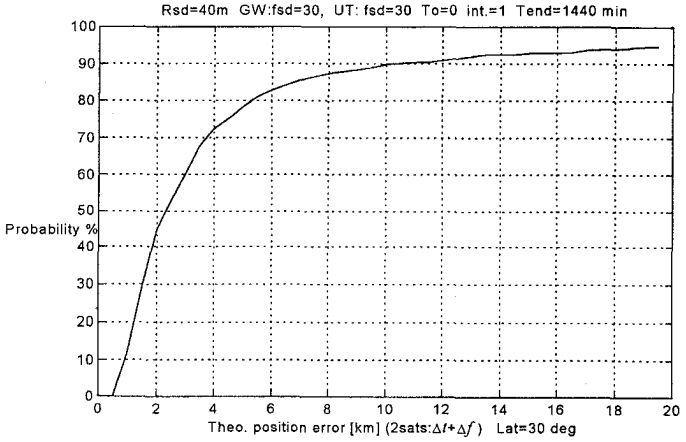

Fig. 12. CDF of theoretical STD of passive-positioning error using two satellites.

20 km). Recall that in two-satellite *active* positioning, there were no GDOP singularities, and the median error was 0.3 km. However, as was pointed out in Section IVB, time is not as critical in passive positioning. Hence, the UT can determine the GDOP and repeat the passive positioning process until a good GDOP is detected. Another possible use of the available time is to repeat the measurements in order to reduce random position error.

In Fig. 5 we noted qualitatively that in the area of bad GDOP for RTD + Δt (around the baseline) the GDOP of $\Delta t + \Delta f$ is usually good and vice versa. This phenomena is confirmed quantitatively in Fig. 13.

VII. BIAS ERRORS

Errors considered here as *bias* errors (in contrast to random errors) are those errors that will repeat themselves if the position measurements are repeated closely in time. In quick positioning there is no time to repeat the measurements, hence bias errors will affect positioning in a similar way as random errors. If however, measurement will be repeated, bias errors will not average out as would random errors. On the other hand, some bias errors (common to neighboring UTs) could be removed by performing differential corrections obtained with a reference UT at a known location.

There are many sources of bias errors. One source is the error in the assumed *UT height* above the Earth surface model. Its expected effect was analytically derived in Section IIIC with respect to single-satellite positioning. In two-satellite positioning a similar height-induced bias error is expected. We pointed out that height-induced bias error can be reduced by using detailed topographic maps. The positioning algorithm can be repeated using the height associated with the estimated position.

Another source is *satellite position* error. It can be a true error, or a quantization error, caused by the limited message size devoted to the satellite ephemeris dissemination. The most common satellite position error is an along-orbit error. Appendix C shows that an along-orbit satellite position error d_{sat} will result in a single-satellite UT positioning median error d_{UT}

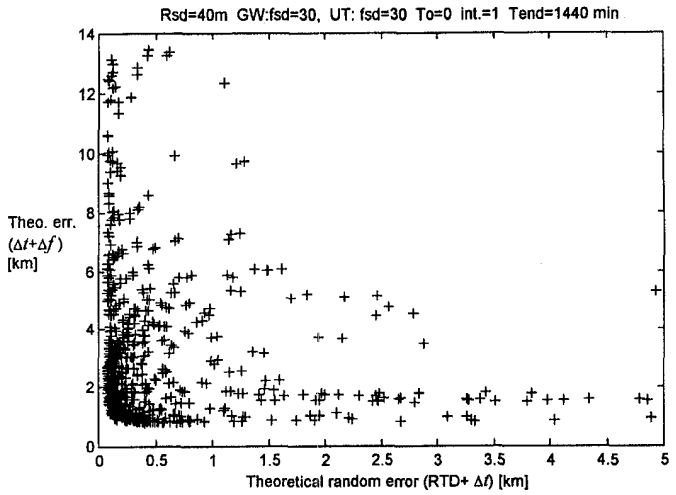

Fig. 13. Negative correlation between GDOP singularities in active and passive positioning.

given by

$$d_{\mathrm{UT}} \approx 2d_{\mathrm{sat}} \frac{R_{\mathrm{E}}}{R_{\mathrm{E}} + h_{\mathrm{sat}}} \tag{20}$$

where R_{E} is the Earth radius and h_{sat} is the satellite height above the Earth surface. The spread around this median error, caused by changing geometry, decreases as the distance between the GW and the UT decreases. For a UT collocated with the GW, the error is always equal to the median. Equation (20) implies that an orbit error of 50 m will result a median position error of 80 m. In two-satellite active positioning, along-orbit error STD of 50 m will result a median UT position error of 0.2 km (statistics obtained for all possible scenarios at 30° latitude). 50 m is the presently assumed worst case error in an orbit predicted by a Globalstar GW using 24 h old ephemeris.

Doppler measurements bring with them more sources of bias error. One source is *satellite frequency error*. If any of the two satellite relays exhibit an unknown frequency error (relative to the nominal frequency), then the error-difference is directly coupled into the Doppler-difference Δf. Similarly, a satellite frequency error affects the RTDop measurement conducted through that satellite. Globalstar's presently specified satellite fractional frequency error STD is 10^{-9}. Such a frequency error will result a median position errors of 0.4 km (single-satellite), 0.05 km (two-satellite active) and 0.8 km (two-satellite passive).

Another frequency related source of bias error results from the conflict between the changing Doppler frequency and the noninstantaneous nature of a frequency measurement. Frequency measurement is effectively an integration of the instantaneous frequency. Frequency measurement can be implemented by measuring the phase change (or cycle count) over a time period τ. Another approach is by reading the control signal of an oscillator in a frequency or phase-locked loop. The time constant of the loop is the equivalent of the integration time τ.

One way to cope with the extended duration of the frequency measurement is to assume linear frequency change, and to associate the measurement with the range-rate at the middle of the measurement duration

$$\int_{t-\tau}^{t} f(x)dx \approx \frac{\tau \dot{R}\left(t - \frac{\tau}{2}\right)}{\lambda} \tag{21}$$

where $\dot{R}$ is the range rate and λ is the wavelength. A more accurate relationship, which makes no assumption on the nature of the Doppler change, is between the integrated frequency and a *range-difference*,

$$\int_{t-\tau}^{t} f(x)dx = \frac{R(t) - R(t-\tau)}{\lambda}. \tag{22}$$

All the sources of bias error discussed so far can be controlled by tighter specifications on hardware and software. Some of them can be mitigated by calibration or differential correction. Ionosphere- and atmosphere-induced errors are relatively small compared with other errors in our application. There is however one major source of bias error, UT velocity, which cannot be ignored, controlled, calibrated, or corrected. It is discussed in the next section.

A. Velocity-Induced Bias Error

A major source of Doppler bias error is *UT velocity*. Doppler caused by UT velocity competes with the desired Doppler caused by satellite velocity. As any other error, this one also depends on geometry. In general a bad GDOP location will also be more sensitive to bias error. In order to get statistics of positioning error due to a source of bias error, the positioning algorithm is allowed to converge, once a

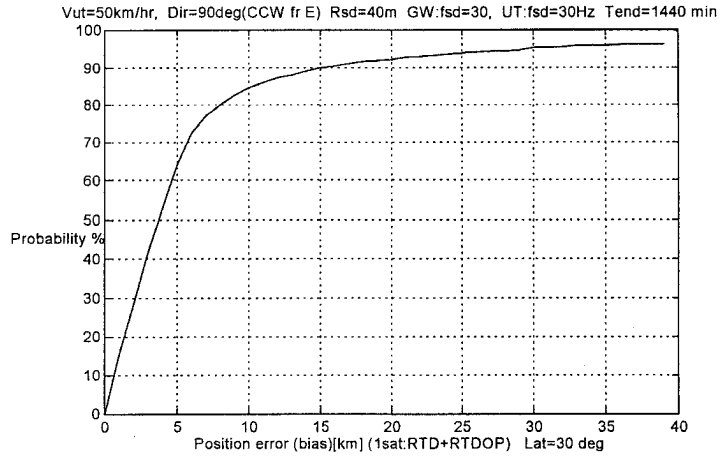

Fig. 14. CDF of 1-sat positioning bias error due to UT velocity of 50 km/h.

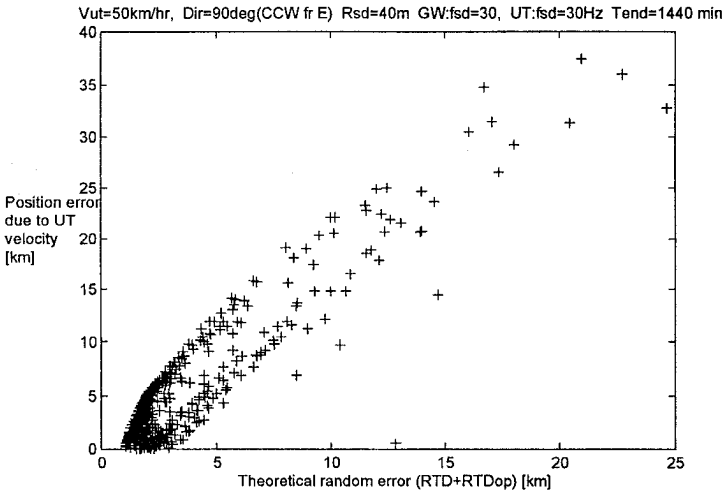

Fig. 15. Correlation between velocity-induced error and theoretical random error (1 satellite).

minute, for 24 h of progressing satellite constellation. Only one bias error source is introduced at each simulation run. Perfect measurements (zero random measurement errors) are used in the simulations, yet the weight matrix **W** is matched to the expected delay (range) and frequency random measurement errors of 40 m and 30 Hz, respectively.

Especially sensitive to velocity error is *single-satellite* positioning. Simulation results of the effect of UT velocity on single-satellite positioning (using RTD and RTDop measurements) are presented in Figs. 14 and 15. A fixed UT velocity of 50 km/h due North was used in all cases. Again, the UT was located at 30° latitude. The bias position error is linearly dependent on the velocity magnitude. In other words, if the velocity would have increased to 100 km/h, the horizontal scales in Fig. 14 would be doubled. With UT velocity of 50 km/h single-satellite positioning exhibits a median bias error of 3.5 km, and in 5% of the single-satellite cases the bias error exceeds 25 km. Directions other than North yielded similar results. It is important to realize that a *two-RTD* positioning (from the same satellite, see Section IIIC) would have suffered from a UT velocity in a very similar way as an RTD + RTDop. Performing two RTD measurements spaced in time, is an equivalent (but slower) way to obtain range and range-rate.

Fig. 15 presents the relationship between the theoretical random error of RTD + RTDop positioning and the velocity-induced bias error. In general there is clear correlation between bad GDOP and high bias error, but the relationship is somewhat complex. Fig. 15 also points out that the bias error induced by a UT velocity of 50 km/h is approximately twice the STD of the random error caused by measurement errors STDs of 40 m (range) and 30 Hz (frequency). Because of the reduced importance of Doppler measurements in *two-satellite* positioning, the velocity-induced bias error becomes much smaller. Fig. 16 indicates that a 50 km/h UT velocity introduces a bias position median error of 50 m, and the error exceeds 3 km in only 2% of the two-satellite cases.

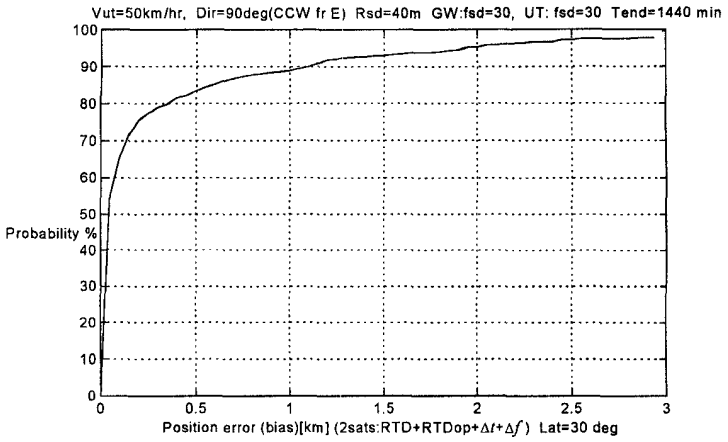

Fig. 16. CDF of 2-sat positioning bias error due to UT velocity of 50 km/h.

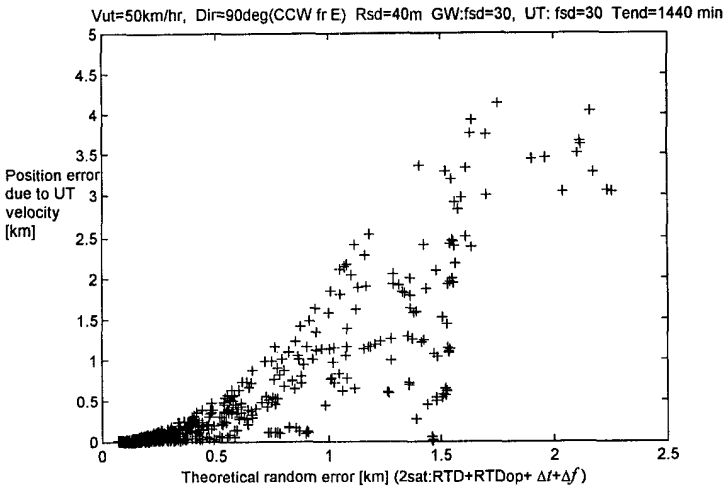

Fig. 17. Correlation between velocity-induced error and theoretical random error (2 satellites).

Fig. 17 presents the relationship between the theoretical random error of two-satellite RTD + RTDop + Δt + Δf positioning and the velocity-induced bias error. An interesting quadratic behavior is noticed. At the more common small theoretical random error (< 0.2 km) the velocity-induced bias error is about 1/5 the theoretical random error, while at the rare geometries yielding large theoretical error (> 1.5 km) the bias error is approximately twice the theoretical random error. This phenomena is attributed to the increasing importance of the Doppler measurements at the relatively bad GDOP locations.

In two-satellite positioning, Doppler-related bias errors (of which the UT velocity is the most important source) can be avoided by utilizing a reduced set of measurements (RTD + Δt). However, at bad GDOP areas, position determination sensitivity to random error, with such a minimal set of measurements, is likely to yield a bigger random error than the velocity-induced bias error. This is clearly demonstrated by comparing Figs. 11 and 17. Fig. 11 shows that when only RTD + Δt are used, the random error can reach 12 km or more (compared with a maximum of 2.3 km when the full set of measurements are used). This is an additional error of approximately 10 km. While Fig. 17 shows that the maximum additional bias error (due to 50 km/h UT velocity) is only 4 km.

To keep this tradeoff issue in perspective, we should recall that two-satellite positioning with the full set of measurements yields a median random error of 300 m and a median bias error of 50 m (due to a UT velocity of 50 km/h). This is so much better accuracy than a single-satellite positioning, that further optimization by judiciously switching between the full set of measurements or a reduced set of measurements is unjustified.

Passive two-satellite positioning was the most sensitive to random measurement error and is also very sensitive to UT velocity. Fig. 18 indicates a median bias error of 7 km, with 5% of the cases suffering an error of more than 60 km.

Fig. 19 demonstrates the correlation between the theoretical random error and the UT velocity-induced bias error. In general the bias error caused by UT

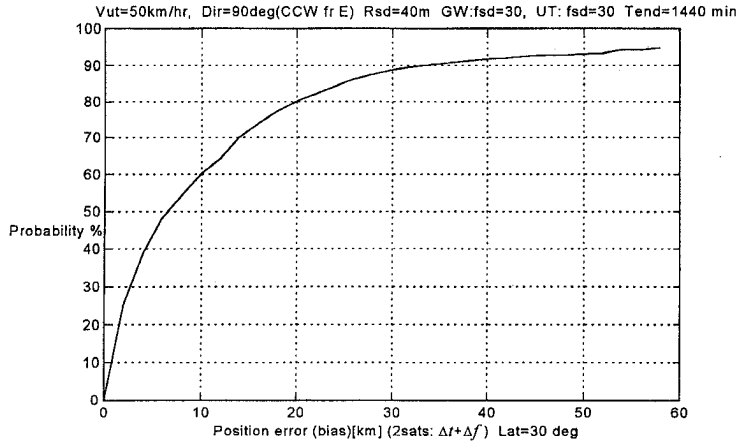

Fig. 18. CDF of 2-sat passive positioning bias error due to UT velocity of 50 km/h.

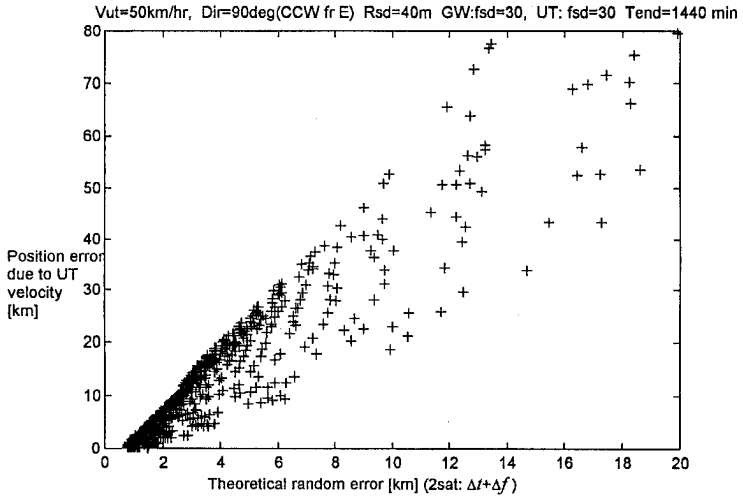

Fig. 19. Correlation between velocity-induced error and theoretical random error (2 sat, passive).

velocity of 50 km/h resulted in an error which is 5 times the theoretical random error. Recall that the theoretical error can be calculated for any specific satellite constellation. Because time is not critical in passive positioning, waiting for a better GDOP situation will also lessen the velocity error.

Finally, the consequences of a velocity-induced error on passive positioning should be considered. A large position error will prompt the UT to reregister. But a fast moving UT needs to register more often anyway. So as long as the interval between distance-based registrations is not allowed to be shorter than some limit, those velocity-induced errors are tolerable.

VIII. CONCLUSIONS

A critical operational need of the Globalstar personal satellite communications system, is a quick, medium accuracy positioning of a user placing a call. We have demonstrated that this requirement can be met using Globalstar's own satellites.

Simulations and analysis demonstrated that combining the unique assets of the Globalstar LEO satellites, makes it possible to obtain quick, medium accuracy positioning of a UT, with one or two satellites. The unique assets are: 1) significant Doppler shift due to the low orbit of the relay satellite, 2) ability to make time and frequency measurements at both ends, the UT and the GW, 3) availability of a two-way communication link to relay the measurements between the two ends, and 4) synchronized time and frequency transmissions from several satellites serving the same GW.

Judiciously exploiting these assets can yield range and range-rate (Doppler) to one satellite. Such information is sufficient to provide 2-D positioning, with two limitation: ambiguity and areas of poor GDOP. A simultaneously received second satellite, when available, adds range-difference and Doppler-difference between the two satellites. This additional information generally resolves ambiguity, and maintains good GDOP almost everywhere. It also results in improved positioning accuracy.

Simulations based on the Globalstar constellation, a UT at mid latitude (30°), and the expected Globalstar measurement errors, indicate the following. 1) Quick 2-D positioning using a single satellite is expected to achieve a random position error smaller than 9 km, in 90% of the cases. 2) Quick 2-D positioning using two satellites is expected to achieve a random position error smaller than 1.4 km, in 90% of the cases. 3) The horizontal position error caused by erroneous height assumption is of the order of the height error. 4) Bias position error due to user velocity of 50 km/h is smaller than 15 km (90%) in single-satellite positioning and 1.2 km (90%) in two-satellite positioning, and the position error is a linear function of the velocity.

These performances meet the operational requirements of the Globalstar system. They are not sufficiently accurate to provide position information to the user himself. The autonomous quick positioning determination of Globalstar is not intended to compete with the high accuracy available from dedicated satellite positioning systems like GPS or GLONASS. However, allowing longer measurement time, and utilizing measurements from reference UTs (at known locations) for differential correction, could improve the positioning accuracy to a degree in which it could serve the user, or those who may need his location.

APPENDIX A. A SIMPLIFIED GLOBALSTAR CONSTELLATION (SPHERICAL EARTH, CIRCULAR ORBITS)

The Earth

$$R_E = 6378 \text{ km}, \quad \text{Earth radius.}$$

The Satellites

$$h_S = 1406 \text{ km}, \quad \text{satellite height}$$

$$R_S = R_E + h_S, \quad \text{radius of satellite orbit}$$

$$\text{incl} = \frac{52}{180}\pi, \quad \text{orbit inclination [radians]}$$

$$\dot{\omega} = \frac{\sqrt{398601.2}}{R_{S\,[\text{km}]}^{3/2}} \text{ rad/s}, \quad \text{orbital velocity}$$

$$\dot{\Omega} = 7.292115856\ 10^{-5} \text{ rad/s},$$

Earth rate of rotation

$$l = 1,2,\ldots,8 \quad \text{(orbit number)}$$

$$m = 1,2,\ldots,6 \quad \text{(satellite number)}$$

$$\omega_0(l,m) = (m-1)\frac{\pi}{3} + (l-1)\frac{\pi}{24}$$

$$\Omega_0(l) = (l-1)\frac{\pi}{4}$$

$$\omega_{l,m}(t) = \omega_0(l,m) + \dot{\omega}t$$

$$\Omega_l(t) = \Omega_0(l) - \dot{\Omega}t.$$

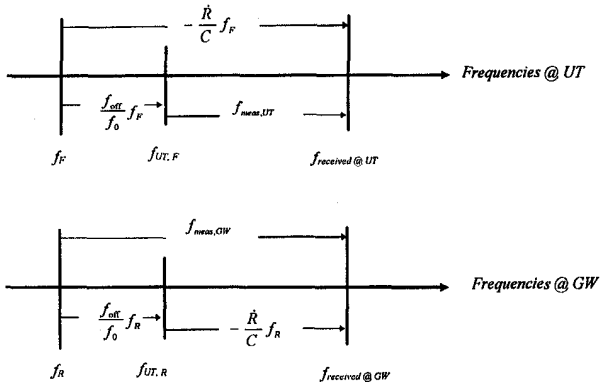

Fig. 20. Relationship between frequencies used to extract round-trip Doppler.

Satellites Cartesian Coordinates (in Earth-centered Earth-fixed coordinate system)

$$x_{l,m}(t) = R_S[\cos(\Omega_l(t))\cos(\omega_{l,m}(t)) - \sin(\Omega_l(t))\sin(\omega_{l,m}(t))\cos(\text{incl})]$$

$$y_{l,m}(t) = R_S[\sin(\Omega_l(t))\cos(\omega_{l,m}(t)) + \cos(\Omega_l(t))\sin(\omega_{l,m}(t))\cos(\text{incl})]$$

$$z_{l,m}(t) = R_S \sin(\omega_{l,m}(t))\sin(\text{incl}).$$

The UT

$$\text{lat,long},h$$

UT Cartesian Coordinates (in Earth-centered Earth-fixed coordinate system)

$$x_{UT} = (R_E + h)\cos(\text{lat})\cos(\text{long})$$

$$y_{UT} = (R_E + h)\cos(\text{lat})\sin(\text{long})$$

$$z_{UT} = (R_E + h)\sin(\text{lat}).$$

The Slant Range Between the UT and Satellite m in Orbit l

$$R_{l,m}(t) = \sqrt{[x_{l,m}(t) - x_{UT}]^2 + [y_{l,m}(t) - y_{UT}]^2 + [z_{l,m}(t) - z_{UT}]^2}.$$

APPENDIX B. ROUND-TRIP-DOPPLER MEASUREMENT

Round-trip Doppler (RTDop) measurement requires separating the UT oscillator offset from the Doppler shift (in the satellite-UT leg). Steven A. Kremm [7] suggested a method to do that when the UT uses the same local oscillator for both transmit and receive. The method is explained with the help of Fig. 20 and the index below. It is assumed that the Doppler shifts in the GW-satellite leg are perfectly known and removed.

- $\dot{R}$ Range-rate of the satellite-to-UT leg,
- C Propagation velocity (speed of light),
- f_F Forward link nominal frequency (2500 MHz),
- f_R Reverse link nominal frequency (1600 MHz),

f_{off}/f_0 Normalized frequency offset of UT's oscillator.

Two measured frequencies are available at the GW: the reported measurement from the UT

$$f_{\text{meas,UT}} = f_F\left(-\frac{\dot{R}}{C} - \frac{f_{\text{off}}}{f_0}\right) \tag{23}$$

and the measurement performed at the GW itself

$$f_{\text{meas,GW}} = f_R\left(-\frac{\dot{R}}{C} + \frac{f_{\text{off}}}{f_0}\right). \tag{24}$$

Adding and subtracting (23) and (24) yields both the UT offset and the range-rate

$$\dot{R} = -\frac{C}{2}\left(\frac{f_{\text{meas,GW}}}{f_R} + \frac{f_{\text{meas,UT}}}{f_F}\right) \tag{25}$$

$$\frac{f_{\text{off}}}{f_0} = \frac{1}{2}\left(\frac{f_{\text{meas,GW}}}{f_R} - \frac{f_{\text{meas,UT}}}{f_F}\right). \tag{26}$$

From (25) we can also obtain the relationship between the frequency measurement errors and the range-rate error. Assuming zero-mean Gaussian frequency errors at the GW and at the UT, with STD of $\sigma_{f,\text{GW}}$ and $\sigma_{f,\text{UT}}$, respectively, then

$$\sigma_{\dot{R}} = \frac{C}{2f_F}\sqrt{\left(\frac{f_F}{f_R}\sigma_{f,\text{GW}}\right)^2 + \sigma_{f,\text{UT}}^2}. \tag{27}$$

APPENDIX C. SINGLE-SATELLITE POSITIONING BIAS ERROR DUE TO SATELLITE ALONG-ORBIT POSITION ERROR

This appendix explains qualitatively the relationship between the along-orbit satellite position error d_{sat} and the resulted UT positioning error d_{UT}, in a single-satellite positioning

$$d_{\text{UT}} \approx 2d_{\text{sat}}\frac{R_{\text{E}}}{R_{\text{E}} + h_{\text{sat}}} \tag{28}$$

where R_{E} is the Earth radius and h_{sat} is the satellite height above the Earth surface. Since this is a single-satellite positioning, if the satellite true position is displaced horizontally d_{sat} from its assumed position, then the solution (the cut between the RTD circle and the RTDop hyperbola on the Earth surface) will simply move with it. However, due to the differences in arc lengths between the satellite orbit circle and the Earth circumference (Fig. 21) the displacement on the Earth surface will be smaller than the satellite displacement by the ratio $R_{\text{E}}/(R_{\text{E}} + h_{\text{sat}})$.

Where does the additional factor of 2 comes from? Consider the **much exaggerated** example in Fig. 22, in which the GW and the true UT position are collocated (point U). The true satellite location is at point S while the assumed satellite location is at point A. The

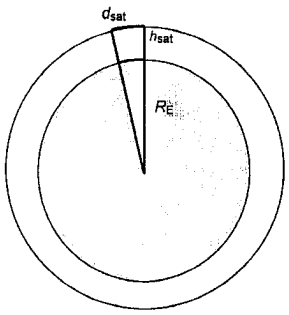

Fig. 21. Geometry of along-orbit satellite position error (a look from the side).

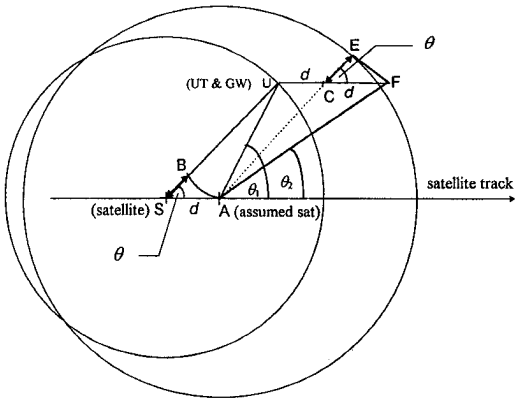

Fig. 22. RTD circles caused by along-orbit satellite position error (a look from above).

figure also assumes that the satellite track is at zero height above a flat Earth surface.

The solved UT position clearly must be on a circle centered at the assumed location of the satellite (point A). We will first show that the circle's radius has to be the distance $\overline{\text{AE}}$. The line AE was drawn parallel to the line US. Hence the triangles UAS and AUC are congruent. The measured "GW-satellite-UT" distance is $2\overline{\text{US}}$

$$2\overline{\text{US}} = \overline{\text{US}} + \overline{\text{UB}} + \overline{\text{BS}}. \tag{29}$$

This is also the used "GW-assumed satellite-calculated UT" distance given by $\overline{\text{UAE}}$. From the fact that the triangles UAS and AUC are congruent, we get

$$\overline{\text{UAE}} = \overline{\text{UA}} + \overline{\text{AC}} + \overline{\text{CE}} = \overline{\text{UB}} + \overline{\text{US}} + \overline{\text{CE}}. \tag{30}$$

Equating (29) and (30) yields

$$\overline{\text{CE}} = \overline{\text{BS}}. \tag{31}$$

Since both d and $\overline{\text{BS}}$ are much smaller than the GW-satellite leg $\overline{\text{US}}$, we can write

$$\overline{\text{CE}} = \overline{\text{BS}} \approx d\cos\theta. \tag{32}$$

The point F is at a distance $2d$ along track from the true UT position. We now show that both E and F are practically on the same circle centered at A, by noting that

$$\overline{\text{AE}} = \overline{\text{AC}} + \overline{\text{CE}} \approx \overline{\text{AC}} + d\cos\theta \tag{33}$$

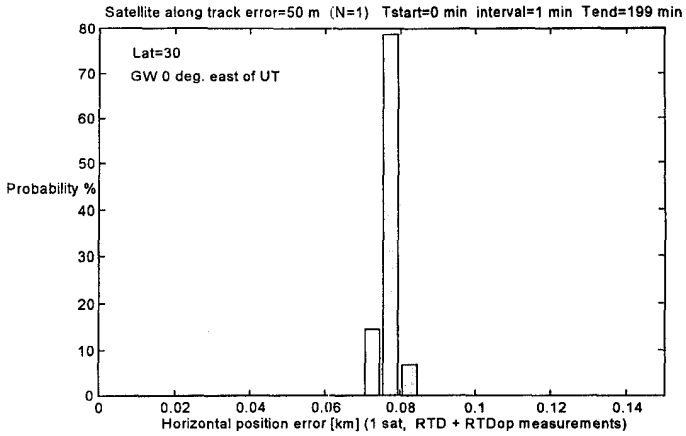

Fig. 23. UT position error due to 50 m along-orbit satellite error (UT collocated with GW).

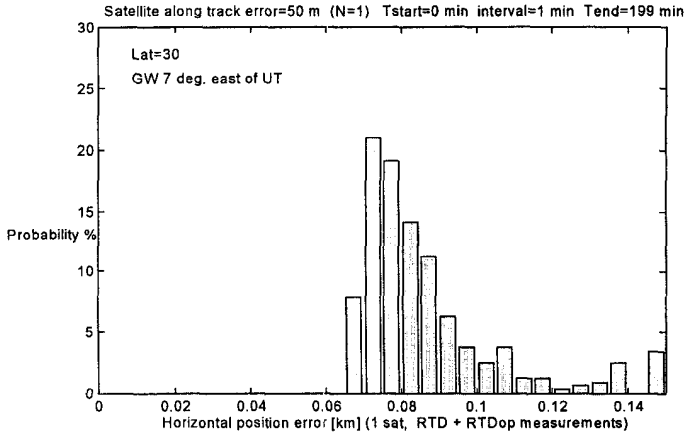

Fig. 24. UT position error due to 50 m along-orbit satellite error (UT 7° West of GW).

and

$$\overline{\mathrm{AF}} = \sqrt{(\overline{\mathrm{AC}})^2 + d^2 - 2\overline{\mathrm{AC}}d\cos(180-\theta)}$$

$$\approx \overline{\mathrm{AC}} + d\cos\theta \tag{34}$$

$$\therefore\ \overline{\mathrm{AF}} \approx \overline{\mathrm{AE}}. \tag{35}$$

To complete the proof that the solved UT position is at point F and not anywhere else on the larger circle, we need to satisfy the Doppler measurement, which requires that

$$\cos\theta_2 = 2\cos\theta - \cos\theta_1 \tag{36}$$

namely we need to show that

$$\frac{\overline{\mathrm{US}}\cos\theta + d}{\overline{\mathrm{US}} + d\cos\theta} = 2\cos\theta - \frac{\overline{\mathrm{US}}\cos\theta - d}{\overline{\mathrm{US}} - d\cos\theta}; \qquad d \ll \overline{\mathrm{US}}. \tag{37}$$

It is straight forward to show that (37) is indeed correct when $d \ll \overline{\mathrm{US}}$.

Equation (28) predicts that a 50 m along-orbit satellite position error will cause an 80 m UT position error. Simulation results, for a single-satellite positioning of a UT collocated with the GW (Fig. 23), confirm this predicted error. The simulation were conducted for 200 min of changing satellite constellation, relative to a UT at 30° latitude. When there is a significant distance between the GW and the UT, the geometry becomes more complex and there is no simple relationship between d_{sat} and d_{UT}. The simulation results in Fig. 24, which pertain to a spacing of 7° longitude between the UT and the GW, demonstrate a spread in the resulting UT position error, with a median still near the predicted error of 80 m.

ACKNOWLEDGMENT

The author is indebted to W. G. Ames, J. Determan, S. Vembu, E. B. Victor, and the late G. Skinner for many valuable and stimulating discussions. The author would also like to thank A. J. Viterbi for providing a sabbatical appointment at Qualcomm Inc.

REFERENCES

[1] Hirshfield, E. (1995)
The Globalstar System.
Applied Microwave and Wireless (Summer 1995), 26–41.

[2] Parkinson, B. W., Stansell, T., Beard, R., and Gromov, K. (1995)
A history of satellite navigation.
Navigation, **42**, 1 (1995), 109–164.

[3] Bessis, J. L. (1981)
Operational data collection and platform location by satellite.
Remote Sensing of the Environment, **11**, 2 (May 1981), 93–111.

[4] Ames, W. G. (1990)
A description of Qualcomm automatic satellite position reporting (QASPR) for mobile communications.
In *Proceedings of the 2nd International Mobile Satellite Conference*, Ottawa, June 1990, 285–290.

[5] Colcy, J. N., Hall, G., and Steinhauser, R. (1995)
Euteltracs: The European mobile satellite service.
Electronics and Communication Engineering Journal (Apr. 1995), 81–88.

[6] Kimura, K., Morikawa, E., Kozono, O., and Wakana, H. (1996)
Communication and radio determination system using two geostationary satellites, Part II: Analysis of positioning accuracy.
IEEE Transactions on Aerospace and Electronic Systems, **32**, 1 (Jan. 1996), 314–325.

[7] Kremm, S. A. (1995)
Personal communication.

[8] Sorenson, H. W. (1980)
Parameter Estimation—Principles and Problems.
New York: Marcel Dekker, 1980.

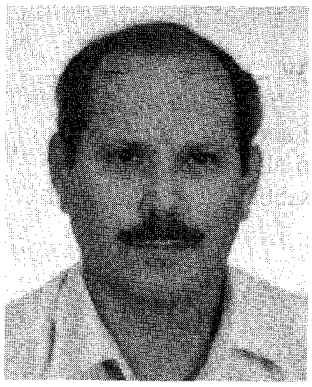

Nadav Levanon (S'67—M'69—SM'83—F'98) was born in Israel in 1940. He received the B.Sc. and M.Sc. in electrical engineering from the Technion–Israel Institute of Technology, Haifa, in 1961 and 1965, respectively, and the Ph.D. in electrical engineering from the University of Wisconsin, Madison, in 1969.

From 1961 to 1965 he served in the Israeli Army. He has been a faculty member at Tel-Aviv University since 1970, first in the Department of Geophysics, and since 1977 in the Department of Electrical Engineering–Systems, where he is a Professor. He was Chairman of that department from 1983 to 1985. He was a Visiting Associate Professor at the University of Wisconsin, from 1972 to 1974, and a Visiting Scientist at The Johns Hopkins University, Applied Physics Laboratory, in the academic year 1982–1983. From 1994 to 1996 he was a Principal Engineer at Qualcomm Inc., San Diego.

Dr. Levanon is the author of the book *Radar Principles* (Wiley, 1988).